

FULL-WAVE ANALYSIS OF COUPLED WAVEGUIDES IN A TWO-DIMENSIONAL PHOTONIC CRYSTAL

Z. G. Kashani, N. Hojjat, and M. Shahabadi

Department of Electrical and Computer Engineering
University of Tehran
Tehran, Iran

Abstract—It is shown that the modal analysis of coupled waveguides in a two-dimensional photonic crystal can be reduced to the evaluation of natural frequencies of an equivalent network. This network is constituted of ideal transmission lines and transformers and is directly derived from Maxwell's equations without any simplifying assumptions. The natural frequencies of the proposed equivalent network are computed after its subdivision into a series of cascaded sub-networks. These sub-networks are then described by their multi-port impedance matrices so that the entire network can be described by the cascaded connection of these matrices. Resonance conditions of this cascaded connection yield the natural frequencies and consequently the propagation constants of various modes of the original coupled photonic-crystal waveguides. Under the resonance condition, the voltages and currents of the equivalent network are nonzero, and they can be used to determine all the field components of the corresponding mode. The obtained numerical results verify the fact that the coupling length of photonic-crystal directional couplers can be reduced considerably.

1 Introduction

2 Method of Analysis

3 Numerical Results

4 Conclusions

Acknowledgment

References

1. INTRODUCTION

Optical directional couplers play a major role in many telecommunication subsystems such as intensity modulators, switches, and power dividers [1]. An optical directional coupler is commonly composed of two parallel dielectric waveguides whose modal fields are coupled. As a result of this coupling, electromagnetic waves propagating along one waveguide excite modes of the neighboring waveguide, thus power coupling takes place. Among different methods for implementing optical directional couplers [2–5], those in which optical waveguides are implemented using periodic dielectric structures have found great attention. For the same token, photonic-crystal waveguides can be exploited in implementation of optical couplers. A photonic-crystal waveguide is realized by introducing a linear defect in a bulk photonic crystal. In other words, a photonic-crystal waveguide resembles a hollow waveguide with walls made of a photonic crystal. In the bandgap of these walls, electromagnetic waves propagate along the waveguide because of the total reflection at its walls.

The first implementation of a two-dimensional (2-D) photonic-crystal coupled waveguide has been reported in [4]. There, by inserting two parallel linear defects in a bulk photonic crystal, a directional coupler has been constructed. Along a so-named coupling length, the linear defects, i.e., waveguides, are in close proximity where the mutual coupling can take place. It is important to note that the space between the two waveguides of a photonic-crystal coupler is also filled by a photonic crystal whereas for conventional optical couplers this space is filled by a homogeneous medium. By changing either the coupling length or the number of layers placed between the two waveguides, one can achieve a specific coupling coefficient. In most cases, even a short coupling length leads to any desired coupling coefficient, as a result of which implementation of compact devices is made possible [5].

The behavior of photonic-crystal directional couplers has been studied by various computational methods such as the plane-wave expansion (PWE) method [7] and the time-domain beam propagation method (BPM) [4]. To analyze photonic-crystal couplers with the help of the PWE method, one should exploit the concept of super-cell. To this end, the two linear defects corresponding to the two coupled waveguides must be repeated periodically prior to the application of the PWE analysis since the PWE method is merely applicable to periodic structures. But as the dimensions of the super-cell are larger than those of the original waveguides, the computation time required for the PWE analysis of photonic-crystal couplers is greater than the corresponding analysis for a bulk photonic crystal. Note

that the larger the dimensions of the super-cell, the larger will be the number of the required plane waves for the PWE analysis. As will be discussed shortly, the method of this paper is not based on the concept of super-cell and thus is computationally more efficient because the number of required spatial harmonics can be maintained very small. In contrast to the time-domain BPM, the method of this work does not make use of any perfectly matched layer (PML) nor is there any spatial discretization involved. Therefore, in our method the geometrical features of the structure can be taken into account with higher accuracy.

In the present work, a combination of a network model [8, 9] and the transverse resonance technique is used to analyze photonic-crystal couplers. With the help of this method, the modal analysis of a 2-D photonic-crystal coupled waveguide can be reduced to the evaluation of the natural frequencies of an equivalent network composed of transmission lines. Moreover, the proposed method provides us with a physical insight into the coupling mechanism.

This paper is organized as follows. In Section 2, the equivalent network of two coupled photonic-crystal waveguides is developed. In Section 3, using the developed model, the propagation constants of the guided modes and consequently the coupling length of a photonic-crystal coupler are evaluated. Some brief concluding remarks are presented in Section 4.

2. METHOD OF ANALYSIS

Fig. 1 depicts a coupler structure implemented in a 2-D square lattice of parallel infinite dielectric rods surrounded by air. The rods are assumed to have square cross-section and be parallel to the z axis. Two parallel waveguides of width W are formed by introducing two line defects in the crystal. As the goal of analysis, the propagation constants of the coupled guided modes and their corresponding field distributions are to be determined.

It should be noted that in this article, our discussion is focused on TM polarization because square-rod structures show bandgap exclusively for TM_z modes [10].

Fig. 2 illustrates one of the rows of the photonic crystal shown in Fig. 1. In Region 2 of Fig. 2, called periodic region, the relative permittivity $\varepsilon_r(x)$ is a periodic function of x ; it can thus be expanded using the following Fourier series

$$\varepsilon_r(x) = \lim_{N \rightarrow \infty} \sum_{n=-N}^N \tilde{\varepsilon}_n e^{-j2n\pi x/L_x}, \quad (1)$$

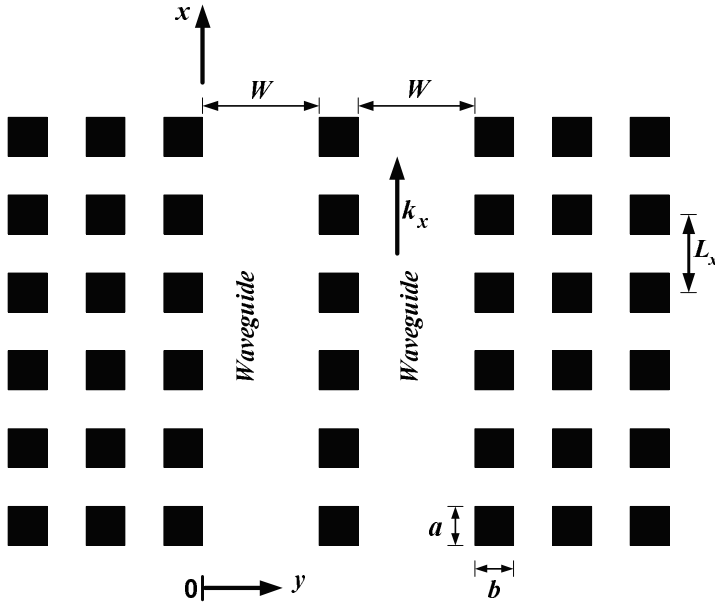


Figure 1. A photonic-crystal waveguide coupler with one row of dielectric rods in the coupling region.

in which L_x is the lattice constant in the x -direction and

$$\tilde{\varepsilon}_n = \frac{1}{L_x} \int_0^{L_x} \varepsilon_r(x) e^{j2n\pi x/L_x} dx. \quad (2)$$

In addition, the total TM_z field in the periodic region is pseudo-periodic, so the E_z and H_x components of this field are given by

$$E_z(x, y) = \lim_{N \rightarrow \infty} \sum_{n=-N}^N E_{z_n}(y) e^{-j\alpha_n x} \quad (3)$$

$$H_x(x, y) = \lim_{N \rightarrow \infty} \sum_{n=-N}^N H_{x_n}(y) e^{-j\alpha_n x}, \quad (4)$$

where $\alpha_n = k_x + 2n\pi/L_x$ in which k_x is the unknown propagation constant along the x -direction. After elimination of H_y , Maxwell's equations for the components of the TM_z field will lead to

$$\frac{\partial}{\partial y} E_z = -j\omega\mu_0 H_x$$

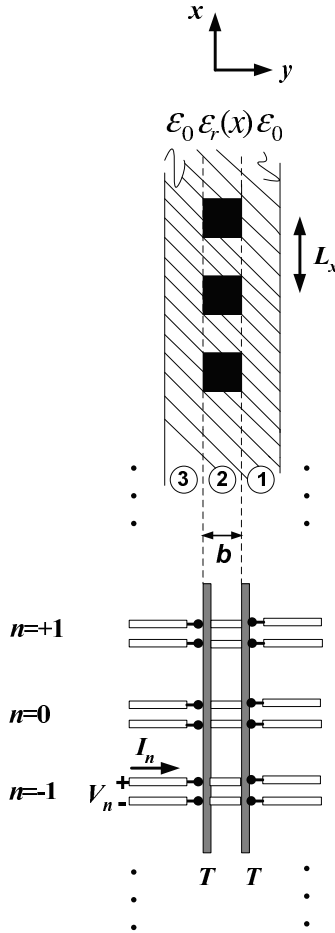


Figure 2. Network model for a rectangular periodic structure. The line voltages V_n and currents I_n correspond to E_{z_n} and H_{x_n} , respectively.

$$\frac{\partial}{\partial y} H_x = -j\omega\epsilon_0 \left(\epsilon_r(x) + \frac{1}{\omega^2\mu_0\epsilon_0} \frac{\partial^2}{\partial x^2} \right) E_z$$

which is a system of differential equations with partial derivatives of the first order. Here, the working frequency is assumed to be ω . Substituting (1), (3), and (4) in the above system, one easily arrives

at

$$\begin{aligned} \sum_{n=-N}^N \frac{d}{dy} E_{z_n}(y) e^{-j\alpha_n x} &= -j\omega\mu_0 \sum_{n=-N}^N H_{x_n}(y) e^{-\alpha_n x} \\ \sum_{n=-N}^N \frac{d}{dy} H_{x_n}(y) e^{-j\alpha_n x} &= \\ -j\omega\varepsilon_0 \sum_{n=-N}^N \left(\sum_{m=-N}^N \tilde{\varepsilon}_{n-m} E_{z_m}(y) - \frac{\alpha_n^2}{\omega^2\mu_0\varepsilon_0} E_{z_n}(y) \right) &e^{-j\alpha_n x}. \end{aligned}$$

Since the exponential functions $\exp(-j\alpha_n x)$ form a complete set of basis functions, the above system of equations holds if and only if the corresponding coefficients in the above linear combinations are equal. By equating the corresponding coefficients, the following system of first-order differential equations will be obtained:

$$\frac{d}{dy} \begin{pmatrix} \dots \\ E_{z_{n-1}}(y) \\ E_{z_n}(y) \\ \dots \end{pmatrix} = -j\omega\mu_0 \begin{pmatrix} \dots \\ H_{x_{n-1}}(y) \\ H_{x_n}(y) \\ \dots \end{pmatrix} \tag{5}$$

$$\frac{d}{dy} \begin{pmatrix} \dots \\ H_{x_{n-1}}(y) \\ H_{x_n}(y) \\ \dots \end{pmatrix} = -j\omega\varepsilon_0([N^2] - [\alpha]^2/k_o^2) \begin{pmatrix} \dots \\ E_{z_{n-1}}(y) \\ E_{z_n}(y) \\ \dots \end{pmatrix} \tag{6}$$

in which

$$[N^2] = \begin{bmatrix} & & \dots & & \\ & \tilde{\varepsilon}_o & \tilde{\varepsilon}_{-1} & \tilde{\varepsilon}_{-2} & \\ \dots & \tilde{\varepsilon}_1 & \tilde{\varepsilon}_o & \tilde{\varepsilon}_{-1} & \dots \\ & \tilde{\varepsilon}_2 & \tilde{\varepsilon}_1 & \tilde{\varepsilon}_o & \\ & & \dots & & \end{bmatrix}, \tag{7}$$

$k_o = \omega\sqrt{\mu_o\varepsilon_o}$, and $[\alpha]$ is a $(2N + 1) \times (2N + 1)$ diagonal matrix whose diagonal elements are α_n . It is observed that (5) and (6) are similar to the equations governing a multi-conductor transmission line provided that (E_{z_n}, H_{x_n}) is considered as the voltage-current pair of the n -th transmission line. Note that (5) and (6) are also valid in a homogeneous region, such as Region 1 and 3 in Fig. 2, where the relative permittivity assumes a constant value independent of x . In the periodic region, because of the nondiagonal elements of $[N^2]$ the above transmission lines are mutually coupled whereas in the homogeneous regions the matrix $[N^2]$ is diagonal and the transmission lines are decoupled.

In conformity with transmission-line equations, the substitutions

$$[V(y)] = [\cdots, E_{z_{n-1}}(y), E_{z_n}(y), \cdots]^T \quad (8)$$

$$[I(y)] = [\cdots, H_{x_{n-1}}(y), H_{x_n}(y), \cdots]^T \quad (9)$$

$$[C] = \varepsilon_o([N^2 - [\alpha]^2/k_o^2]) \quad (10)$$

$$[L] = \mu_o[\mathbf{1}] \quad (11)$$

are used. These will transform (5) and (6) into

$$\begin{cases} \frac{d}{dy}[V(y)] &= -j\omega[L][I(y)] \\ \frac{d}{dy}[I(y)] &= -j\omega[C][V(y)] \end{cases} \quad (12)$$

The above system of first-order differential equations is a rigorous formulation valid for *all the regions* of the structure shown in Fig. 1. Knowing the geometrical and electrical properties of the dielectric rods, one may determine the matrices $[L]$ and $[C]$ from (2), (7), (10), and (11) for every region. It is worth mentioning that the boundary conditions at the interface of two succeeding regions are fulfilled if and only if the continuity of the vectors $[V(y)]$ and $[I(y)]$ is achieved. This is because they correspond to the tangential components of the electric and magnetic field. In summary, solving the equations given by (12) along with the boundary condition of continuity of $[V(y)]$ and $[I(y)]$ for every y leads to the rigorous solution of the original problem.

Now, the solution to the above system of first-order differential equations for a given $[L]$ and $[C]$ is an exponential function, therefore, in accordance to [11], we suggest the following solutions for $[V]$ and $[I]$:

$$[V(y)] = [p]e^{-jk_y y} \quad (13)$$

$$[I(y)] = [q]e^{-jk_y y}. \quad (14)$$

In (13) and (14), $[p]$ and $[q]$ are constant vectors, and k_y is the propagation constant to be determined. By substituting (13) and (14) in (12), the following equations are obtained:

$$-jk_y[p] = -j\omega[L][q] \quad (15)$$

$$-jk_y[q] = -j\omega[C][p]. \quad (16)$$

Substitution of (16) in (15) yields

$$(\omega^2[L][C] - k_y^2[\mathbf{1}])[p] = 0. \quad (17)$$

The above equation will have a non-zero solution if and only if k_y satisfies

$$\det(\omega^2[L][C] - k_y^2[\mathbf{1}]) = 0. \quad (18)$$

From (18), it is obvious that k_y is the eigenvalue of the matrix $\omega^2[L][C]$. Note that if k_y is an eigenvalue of $\omega^2[L][C]$, so is $-k_y$. If we denote the n -th eigenvalue by k_{y_n} , the corresponding eigenvector $[p_n]$ can be evaluated from (17). Obviously, there are $2N + 1$ eigenvalues and eigenvectors.

Having determined all k_{y_n} and $[p_n]$ for Region 2 of Fig. 2, we may, according to [11], obtain the complete solution for $[V(y)]$ as

$$[V(y)] = \sum_n (\tilde{V}_n^+ e^{-jk_{y_n}y} + \tilde{V}_n^- e^{-jk_{y_n}(b-y)}) [p_n] \quad (19)$$

or

$$[V(y)] = [P][\tilde{V}(y)] \quad (20)$$

in which

$$[P] = [\cdots |[p_n]| [p_{n+1}] | \cdots], \quad (21)$$

$$[\tilde{V}(y)] = (\cdots, \tilde{V}_n(y), \tilde{V}_{n+1}(y), \cdots)^T, \quad (22)$$

and $\tilde{V}_n(y)$ is defined as

$$\tilde{V}_n(y) = \tilde{V}_n^+ e^{-jk_{y_n}y} + \tilde{V}_n^- e^{-jk_{y_n}(b-y)}. \quad (23)$$

In the above relations, \tilde{V}_n^+ and \tilde{V}_n^- can be interpreted as the complex amplitude of the n -th forward and backward wave in the y -direction, respectively, and b represents the y -dimension of the region under investigation.

Similarly, $[I(y)]$ can be obtained from

$$[I(y)] = \sum_n (\tilde{I}_n^+ e^{-jk_{y_n}y} + \tilde{I}_n^- e^{-jk_{y_n}(b-y)}) [q_n] \quad (24)$$

or

$$[I(y)] = [Q][\tilde{I}(y)] \quad (25)$$

in which

$$[Q] = [\cdots |[q_n]| [q_{n+1}] | \cdots] = \omega[C][P][k_y]^{-1}, \quad (26)$$

and

$$[\tilde{I}(y)] = (\cdots, \tilde{I}_n(y), \tilde{I}_{n+1}(y), \cdots)^T. \quad (27)$$

Again $\tilde{I}_n(y)$ is given by

$$\tilde{I}_n(y) = \tilde{I}_n^+ e^{-jk_{y_n}y} + \tilde{I}_n^- e^{-jk_{y_n}(b-y)}. \quad (28)$$

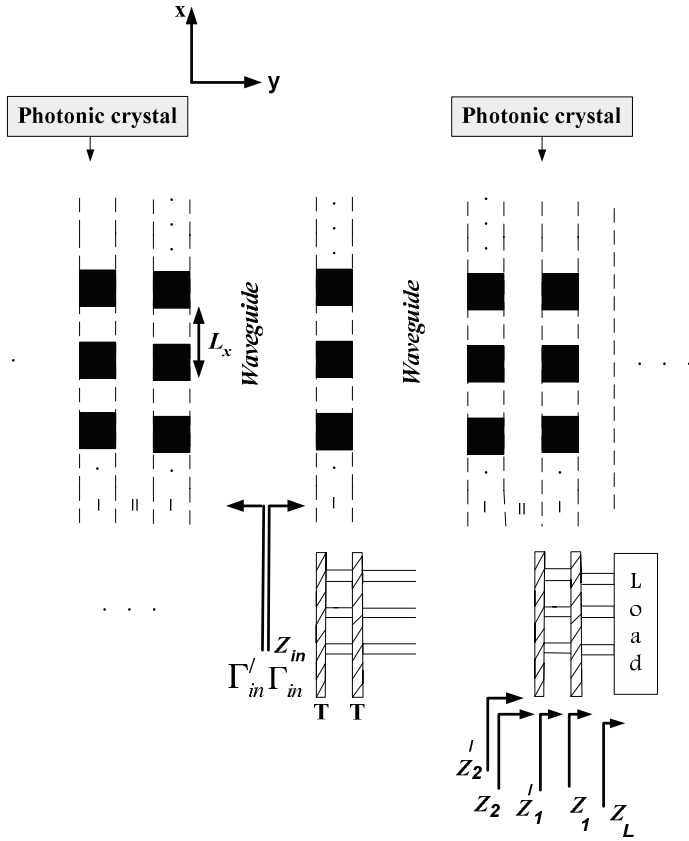


Figure 3. The network model of two coupled photonic-crystal waveguides.

Note that (19) and (24) are solutions to (12) for both a periodic region, e.g., Region 2 of Fig. 2, and a homogeneous layer, e.g. Region 1 in the same figure. Since k_{y_n} are different for homogeneous and periodic layers, the continuity of $[V(y)]$ and $[I(y)]$ at the interface of two neighboring layers must be achieved with the help of a transformer [8]. This is depicted in Fig. 2 by the multi-port network T .

In summary, the wave propagation in the coupled waveguide of Fig. 1 can be modeled by the equivalent network of Fig. 3 in which $2N + 1$ decoupled transmission lines simultaneously model (19) and (24) for each layer while the transformers T at the interface of different layers model the necessary boundary conditions. It can be shown that each transformer T will transform the impedance $[Z]$ seen to the right

of an interface into the impedance $[\tilde{Z}]$ given by

$$[\tilde{Z}] = [P]^{-1}[Z][Q] \quad (29)$$

where $[P]$ and $[Q]$ are defined by (21) and (26), respectively.

After modeling the coupled waveguides using the above mentioned transmission lines and transformers, in order to find the bandgap of photonic-crystal walls, we calculate $[Z_{in}]$ in the doped region, i.e. waveguide region of Fig. 3. For this purpose, we terminate the equivalent network with an impedance $[Z_L]$. The value of this impedance could be chosen arbitrarily. The reason is that in the bandgap of the photonic crystal, electromagnetic waves cannot propagate within the photonic crystal, therefore the value of the load does not affect $[Z_{in}]$. By applying the well-known methods of transmission-line theory, the input impedance is calculated for the successive layers of the network. Multiple transformation of $[Z_L]$ through a relatively large number of periodic layers will provide us with a good estimation of $[Z_{in}]$ in the waveguide region. Note that $[Z_{in}]$ will be reactive as the photonic-crystal walls are operating in their bandgap frequencies.

Using $[Z_{in}]$, we can evaluate the corresponding reflection matrix $[\Gamma_{in}]$. The same procedure must be followed to determine the reflection matrix $[\Gamma'_{in}]$ looking to the left (see Fig. 3). If the matrices $[\Gamma_{in}]$ and $[\Gamma'_{in}]$ satisfy

$$\det([\Gamma_{in}][\Gamma'_{in}] - [1]) = 0 \quad (30)$$

for a specific k_x at a given angular frequency ω , the transverse resonance condition is fulfilled. In other words, all values of k_x and ω satisfying (30) will constitute the dispersion diagram of the coupler.

3. NUMERICAL RESULTS

First we consider a photonic-crystal directional coupler composed of dielectric rods in air with lattice constant L_x , as shown in Fig. 1. The rods are of square cross-section with $a = b = 0.4L_x$ and the refraction index of $n = 3.4$. The waveguide width is $W = 1.6L_x$. The common wall of the two waveguides is a row of the above rods. Because of symmetry, there are both even and odd modes at every given frequency. Fig. 4 illustrates the dispersion diagram of the TM guided modes of the coupled waveguides shown in Fig. 1. In Fig. 4, the area between the top and bottom solid lines forms the pseudo-bandgap. The solid line inside this bandgap is the dispersion diagram of the even mode, whereas the dashed line is that of the odd mode computed by the method of this paper. Our results are verified by comparing them with those obtained

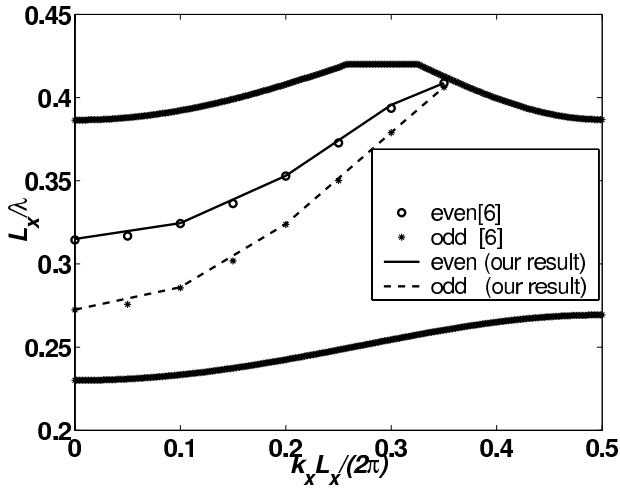


Figure 4. Dispersion diagram for the TM guided modes of the coupled waveguides of Fig. 1.

from an analysis based on the plane-wave expansion method [6]. These are also represented in Fig. 4 by open circles (even modes) and by plus signs (odd modes). As can be seen, they are in good agreement.

The corresponding field distributions along the y -direction are shown in Figs. 5 and 6, where $L_x/\lambda = 0.355$ is assumed in which λ is the free-space wavelength.

As a second example, we consider the coupled waveguides depicted in Fig. 7. Here, the common wall of the two waveguides is constituted of two rows of dielectric rods. The dispersion diagram for these coupled waveguides is illustrated in Fig. 8. Comparing Fig. 4 with Fig. 8, we conclude that a wider common wall leads to a lower coupling and hence to a more equalized propagation constants for even and modes.

The corresponding field distributions for even and odd modes along the y -direction are shown in Fig. 9 and 10, respectively, where $L_x/\lambda = 0.355$.

Fig. 11 demonstrates the coupling length L_c for the directional coupler of Fig. 1 and that of Fig. 7. As can be seen, the coupling length for the directional coupler of Fig. 1 is shorter. This can be explained by the fact that L_c is given by $L_c = 2\pi/|k_e - k_o|$ in which k_e and k_o denote the propagation constant of even and odd mode, respectively.

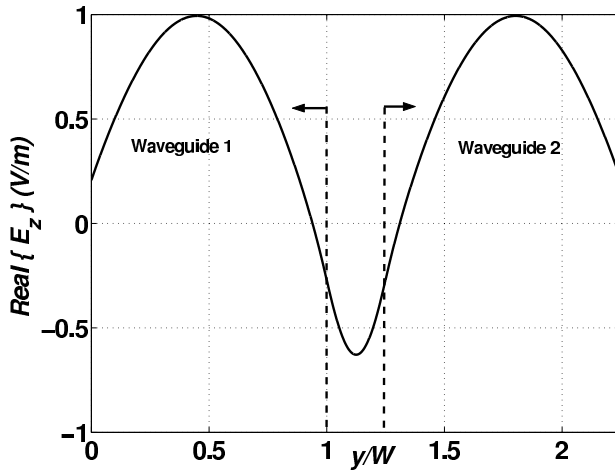


Figure 5. Normalized field pattern for the even mode of the coupler shown in Fig. 1 at $L_x/\lambda = 0.355$.

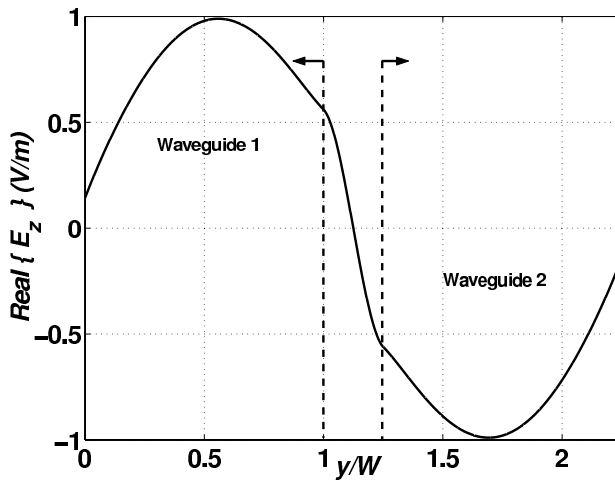


Figure 6. Normalized field pattern for the odd mode of the coupler shown in Fig. 1 $L_x/\lambda = 0.355$.

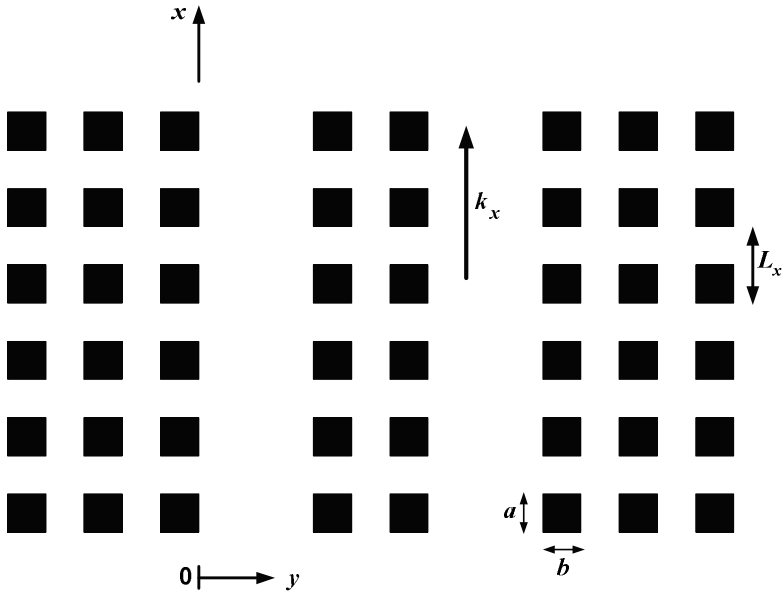


Figure 7. Photonic-crystal waveguide coupler with two rows of dielectric rods in the interaction region.

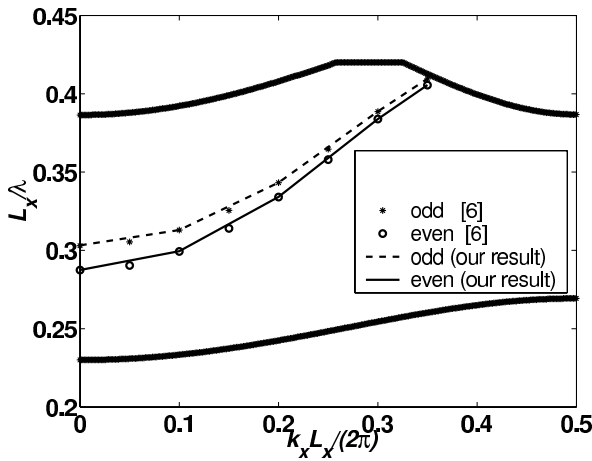


Figure 8. Dispersion diagram for the TM guided modes of the coupled waveguides of Fig. 7.

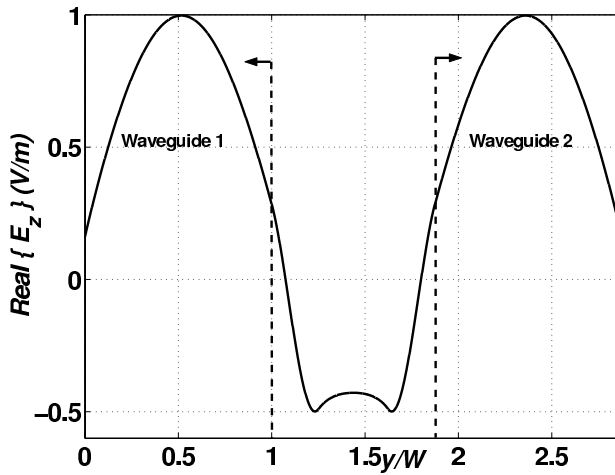


Figure 9. Normalized field pattern for the even mode of the coupler shown in Fig. 7 at $L_x/\lambda = 0.355$.

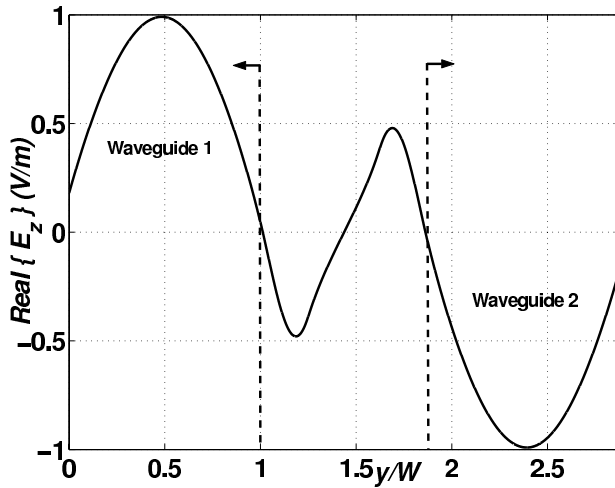


Figure 10. Normalized field pattern for odd mode of the coupler shown in Fig. 7 at $L_x/\lambda = 0.355$.

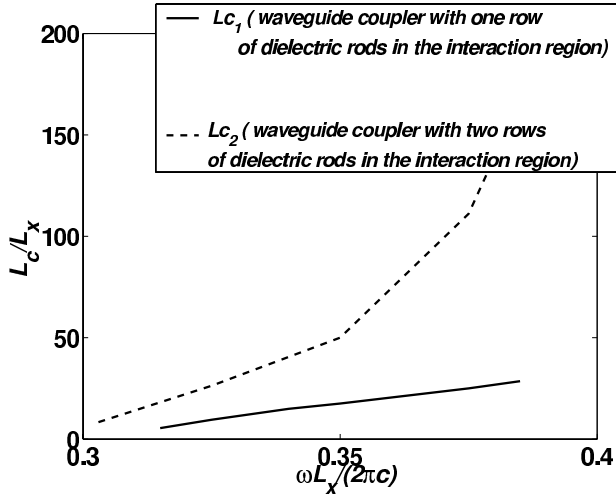


Figure 11. The solid and dashed line represent the coupling length for the photonic-crystal coupler of Figs. 1 and 7, respectively.

4. CONCLUSIONS

Using the introduced matrix formulation, the modal analysis of coupled photonic-crystal waveguides is reduced to the evaluation of natural frequencies of an equivalent network composed of ideal transmission lines and transformers. It has been shown that directional couplers implemented in 2-D photonic crystals can possess very short coupling length because of their relatively large coupling coefficient. These features make them suitable for ultra-compact integrated optical circuits.

ACKNOWLEDGMENT

The partial support of Iran Telecommunication Research Center and the Center of Excellence for Applied Electromagnetics of the University of Tehran is gratefully acknowledged.

REFERENCES

1. Snyder, A. W., et al., *Optical Waveguide Theory*, Chapman and Hall, London, U.K., 1995.
2. Vorobeichik, I. and M. Orenstein, "Intermediate-mode-assisted

- optical directional couplers via embedded periodic structure,” *IEEE J. Quantum Electron.*, Vol. 34, 1772–1781, 1998.
3. Yonekura, J., M. Ikeda, and T. Baba, “Analysis of finite 2-D photonic crystal of columns and lightwave devices using the scattering matrix method,” *J. Lightwave Technol.*, Vol. 17, 1500–1508, 1999.
 4. Koshiba, M., “Wavelength division multiplexing and demultiplexing with photonic crystal waveguide couplers,” *J. Lightwave Technol.*, Vol. 19, 1970–1975, 2001.
 5. Martinez, A., F. Cuesta, and J. Marti, “Ultrashort 2-D photonic crystal directional couplers,” *IEEE Photonics Tech. Lett.*, Vol. 15, 694–696, 2003.
 6. Boscolo, S., M. Midrio, and C. G. Someda, “Coupling and decoupling of electromagnetic waves in parallel 2-D photonic crystal waveguides,” *IEEE J. of Quantum Electron.*, Vol. 38, 47–53, 2002.
 7. Kuchinsky, S., V. Y. Golyatin, A. Y. Kutikov, T. R. Pearsall, and D. Nedeljkovic, “Coupling between photonic crystal waveguides,” *IEEE J. of Quantum Electron.*, Vol. 38, 1349–1352, 2002.
 8. Shahabadi, M. and K. Schünemann, “Millimeter-wave holographic power splitting/combining,” *IEEE Trans. Microwave Theory Tech.*, Vol. 45, No. 12, 2316–2323, 1997.
 9. Shahabadi, M., S. Atakaramians, and N. Hojjat, “Transmission line formulation for the full-wave analysis of two-dimensional dielectric photonic crystals,” to appear in *IEE Proc.*
 10. Joannopoulos, J. D., R. D. Meade, and J. N. Winn, *Photonic Crystals: Molding the Flow of Light*, Princeton Univ. Press, Princeton, NJ, 1995.
 11. Shahabadi, M., “Application of holography to millimeter-wave power combining,” Ph.D. Dissertation, Technische Universität Hamburg-Harburg, 1998 (in German).

Zahra Ghattan Kashani was born in 1979. She received the B.Sc. and M.Sc. degrees from the University of Tehran, Iran, all in electrical engineering in 2002 and 2004, respectively. She has contributed to various research projects in the University of Tehran in the field of microwave and antenna engineering. Her current research interests include photonic crystals and their applications in microwave and millimeter-wave engineering.

Nasrin Hojjat received the B.S.E.E., M.S.E.E., and Ph.D. degrees from the University of Tehran, Iran, all in electrical engineering in 1989, 1991, and 1997, respectively. In 1994 and 1998, she was, respectively, a visiting scholar and a postdoctoral fellow with the Department of Electrical and Computer Eng., University of Waterloo, Canada. In 1991 she joined the Department of Electrical and Computer Engineering, University of Tehran, Iran, as a faculty member. Her primary research interests are numerical methods in electromagnetics, printed circuit analysis, photonic crystals, and smart antennas.

Mahmoud Shahabadi received the B.Sc. and M.Sc. degrees from the University of Tehran, Iran, and the Ph.D. degree from Technische Universitaet Hamburg-Harburg, Germany, all in electrical engineering in 1988, 1991, and 1998, respectively. Since 1998, he has been an Assistant Professor with the Department of Electrical and Computer Engineering, University of Tehran, and since 2002 a Visiting Assistant Professor with the Department of Electrical and Computer Engineering, University of Waterloo, Canada. His research interests and activities encompass various areas of microwave and millimeter-wave engineering as well as photonics. Computational electromagnetics for microwave engineering and photonics find his special interest. He is currently conducting several research projects in the field of antenna engineering, photonic crystals, left-handed materials, and holography. Dr. Shahabadi was awarded the 1998/1999 Price of the German Metal and Electrical Industry, Nordmetall, for the best Ph.D. thesis.